

Review Article

Advanced and Prospects in Toluene Removals

Ho Soonmin¹, Md Shahinoor Islam², Hridoy Roy³

¹Faculty of Health and Life Sciences, INTI International University, Putra Nilai, Negeri Sembilan, Malaysia.

^{2,3}Department of Chemical Engineering, Bangladesh University of Engineering and Technology, Dhaka, Bangladesh.

¹Corresponding Author : soonmin.ho@newinti.edu.my

Received: 10 August 2024

Revised: 11 December 2024

Accepted: 11 February 2025

Published: 28 March 2025

Abstract - Formulated as $C_6H_5CH_3$, toluene is a substituted aromatic hydrocarbon. It is a colorless liquid insoluble in water and smells like paint thinner. Toluene exposure can lead to irritation of the nose and eyes, fatigue, nerve damage, skin inflammation, and damage to the liver and kidneys. The adsorption process has many benefits, including the ability to be reused, in addition to its ability to efficiently and economically remove harmful materials from wastewater. In addition, it is more environmentally friendly if compared to conventional methods. A cheap material with unique qualities like high porosity, high specific surface area, and desired surface functionalization is activated carbon. As a result, activated carbon finds many useful uses in water treatment, pollutant removal, and adsorption. Any member of the class of hydrated minerals that include silicon, aluminum, and alkali and alkaline-earth metals is referred to as a "zeolite". Zeolite is a family of microporous, crystalline aluminosilicate materials frequently employed in industry as catalysts and adsorbents. This review report reports on the use of zeolite, fly ash, and activated carbon in the removal of toluene. Freundlich or Langmuir isotherms provided the best fit for the adsorption data. The value of the thermodynamic parameters indicates whether the adsorption process is exothermic or endothermic, spontaneous, and random. The Freundlich model indicates the extent to which a substance will be adsorbed on a solid surface at a specific concentration, grounded in the concept that the adsorption sites on the surface lack uniformity and possess different adsorption energies. The pseudo-second-order kinetic model indicates that the adsorption rate is affected by the interaction among adsorption sites on the surface. In many cases, activated carbon is seen as a superior adsorbent compared to zeolite, especially for eliminating a broader array of organic contaminants and chemicals because of its greater surface area and more adaptable pore configuration. Fly ash is much less expensive than activated carbon, making it a more economical choice as an adsorbent in different applications because of its abundant availability and status as a waste product.

Keywords - Pollution, Wastewater treatment, Activated carbon, Zeolite, Ash, Adsorption, Water purification.

1. Introduction

Adsorption is a fundamental separation process wherein a substance, known as the adsorbate, accumulates on the surface of a solid material called the adsorbent. This adsorption phenomenon occurs in both gas and liquid phases [1, 2]. The adsorption mechanism comprises several forces, starting from van der Waals, electrostatic, π - π interactions, and hydrogen bond (H-bond) etc. However, most adsorption processes predominantly manifested through electrostatic or van der Waals interactions [3, 4]. The adsorption process is considered a selective separation process. The selectivity of adsorption originates from the relative access and strength of surface interactions for different components of solid/liquid, gas/liquid or solid/solid mixtures. The creation of a large internal surface area leads to numerous small-sized pores, influencing the adsorptive properties of the material. Moreover, the surface polarity controls the affinity of adsorbents with polar or nonpolar groups of adsorbates, further influencing the selectivity of the adsorption process

[5]. The adsorption process is intricately connected with the broader realm of physical, biological, and chemical systems and is used in several industrial applications. In particular, adsorption plays a pivotal role in the purification of wastewater [6]. The fundamental advantage of adsorption processes is using solids such as activated carbon and synthetic resins. These materials become very apparent when considering their applicability in challenging industry separation scenarios [7]. For instance, traditional separation methods, e.g., distillation, may struggle with components having similar boiling points, vapor-liquid azeotropes, or low relative volatilities of species [8]. Alternatively, adsorption excels in handling mixtures with low boiling point differences and is particularly effective in dilute systems, offering a high loading of solute [9]. This characteristic proves invaluable when treating dilute systems, where solutions contain low concentrations of the target component [10]. The ability of adsorption to achieve substantial solute loading enhances its efficiency in dealing with scenarios where other separation



techniques may fall short. This attribute is particularly advantageous in industries dealing with solutions requiring concentrated components for further processing or utilization. Moreover, adsorption processes are less energy-intensive than other separation techniques [11]. Therefore, adsorption is a remarkably adaptable separation technique applicable to a wide range of substances and mixtures. In addition, the versatility of adsorption extends beyond mere separation; adsorption processes are also effective in removing impurities, purification, and concentration of desired components [12].

The adsorption process is deemed economical mainly because it usually demands a lower capital investment owing to its straightforward design, readily accessible and often low-cost adsorbent materials, and simplicity of operation. These factors make it a viable option for numerous applications, such as water treatment and air purification, particularly when contrasted with other intricate separation methods. Various easily accessible materials such as activated carbon, zeolites, and even agricultural waste can serve as adsorbent materials. Adsorption systems usually feature a simple design with few intricate components, reducing installation and upkeep expenses. Adsorption is especially efficient at eliminating contaminants, even at low concentrations, making it advantage in situations where high-purity products are necessary. Adsorption processes find extensive economic application in the chemical process industries, with Activated Carbon (AC) standing out as the most used adsorbent. Activated carbon, a versatile adsorbent, has properties that contribute to its efficacy. AC's large specific surface area provides significant adsorption capacity by creating a large internal surface area that leads to numerous small-sized pores between adsorption surfaces [13].

The size and distribution of these micropores play a crucial role in determining the accessibility of adsorbate molecules to the internal surface, influencing the absorptivity of the material. Surface polarity is another vital characteristic of AC, with hydrophilic adsorbents showing affinity for polar substances like water, while hydrophobic adsorbents prefer nonpolar substances such as hydrocarbons [14]. Activated Carbon (AC) is paramount in wastewater treatment, emerging as a cornerstone in the quest for water purification and environmental sustainability [15].

The exceptional adsorption capabilities of AC make it an invaluable asset in addressing the multifaceted challenges posed by contaminated water. AC shows a critical selective ability to adsorb contaminants from wastewater, as it exhibits a high affinity for a diverse array of pollutants found in wastewater [16]. AC can absorb organic compounds, heavy metals, and specific chemicals from wastewater, efficiently removing impurities that would otherwise compromise water quality and violate environmental standards. The versatility of AC in treatment processes is a key advantage, as it can be customized to adsorb specific contaminants based on the

nature and origin of the wastewater [17]. In addition, the sustainability of AC shines through its renewability and reusability.

The regeneration and reuse of AC extends its lifespan, promoting an eco-friendlier approach to wastewater treatment [18]. Its remarkable efficiency in absorbing organic compounds, such as dyes, phenols, and pesticides, found in industrial wastewater underscores its efficacy in tackling complex pollution challenges in the textile, pharmaceutical and chemical industries. Additionally, the removal of odors and colors by AC contributes to both the chemical purity of treated water and aesthetic improvement for a better world [19]. In addition, AC's adaptability, effectiveness, and eco-friendly features make it a linchpin in the pursuit of comprehensive and sustainable solutions for ensuring the cleanliness and purity of water resources [20]. Toluene has the formula of $C_6H_5CH_3$ and is considered a substituted aromatic hydrocarbon. Generally, it could be derived from petrochemical processes [21]. It is a colorless liquid that does not dissolve in water and has an odor like a thinner paint. Exposure to toluene can cause nose and eye irritation [22], nerve damage, fatigue, skin inflammation, and liver and kidney damage. Table 1 shows the global market volume [23] of toluene from 2015 to 2022. It was noted that the volume of toluene reached 31.26 million metric tons in 2022. Global toluene market growth is rapid due to growth in the plastic sector and transportation industry. On the other hand, Table 2 highlights exporters of toluene in 2022 by countries [24]. It is noted that the largest exporters are China, followed by South Korea, Japan, and Belgium.

Table 1. Global market volume of toluene (2015-2022)

Year	Volume (million metric tons)
2015	26.87
2016	27.72
2017	28.58
2018	29.44
2019	30.32
2020	29.19
2021	29.69
2022	31.26

Table 2. Exporters of toluene in 2022 by countries

Country	Exports value
China	\$687M
South Korea	\$506M
Japan	\$293 M
Belgium	\$285 M
Chinese Taipei	\$270 M
Thailand	\$245 M
Singapore	\$110 M
Israel	\$64.5 M
United Arab Emirates	\$61M
Philippines	\$ 58 M
Malaysia	\$40.1 M

This work reviews the removal of toluene using activated carbon, zeolites and fly ash. These adsorbents have many advantages, such as the ability to be reused and the ability to efficiently and economically remove harmful materials from wastewater. Adsorption data were described using the Langmuir model and Freundlich isotherm.

2. Methodology

Article searches were carried out on Scopus, IEEE Xplore, Elsevier, Google Scholar, and Web of Science databases. Several keywords such as toluene, zeolite, activated carbon, fly ash, adsorption, Langmuir model, Freundlich model, Thermodynamic studies, and wastewater treatment were highlighted. Articles published from 2002 to 2025 will be selected.

3. Removal of Toluene Using Activated Carbon

While other raw materials are continuously being researched and developed, carbonaceous raw materials like wood, coconut shells [25], or premium coals are typically used to manufacture activated carbon. Before going through an activation process that opens the microscopic pore structure and imparts the massive surface area needed for purification applications, the raw material is charred (in the absence of oxygen). Although other methods, such as activation with acidic chemicals [26], are used in the carbon industry, the process is typically carried out in a high-temperature kiln with steam present. Because of its enormous surface area, activated carbon can be used in adsorption to remove undesirable impurities from liquid and gas phase streams [27].

In many cases, activated carbon is seen as a superior adsorbent compared to zeolite, especially for eliminating a broader array of organic contaminants and chemicals because of its greater surface area and more adaptable pore configuration. Generally, activated carbon tends to be less expensive than zeolite when examining the expenses of the raw materials and the associated production methods, rendering it a more cost-effective choice in numerous applications, particularly in large-scale water treatment or industrial adsorption processes.

Specifications of commercial activated carbon (Vazin Carbon, Iran) such as size (0.4-1.2 mm), total surface area (900 m²/g), ash content (12%), apparent density (480-500 kg/m³) and moisture (3%) were reported [28]. The highest removal of toluene reached 99.5% in specific conditions (pH=2, contact time=100 minutes, dosage=0.7 g/L, temperature=40 °C and initial concentration=30 mg/L). However, the percentage of uptake was 96.9% for real wastewater samples. Generally, toluene is considered a clear liquid; however, it is converted to vapor when exposed to air. Buckwheat (*Fagopyrum esculentum* Moench) hulls were used to make carbon adsorbents [29] that were intended to extract gaseous toluene from the atmosphere. Potassium carbonate

was used to impregnate raw hull powder, which was then thermally decomposed to create a chemically activated adsorbent. Comparing the adsorbent made without chemical activation to the one prepared with it, the chemically activated adsorbent showed better toluene adsorption capability. Using an un-activated adsorbent, the toluene concentration in the air dropped from 220 ppm to 160 ppm in under 24 hours. After the adsorption utilizing potassium carbonate (K₂CO₃) activated adsorbent under the same circumstances, only a trace amount of toluene remained.

The rationale behind this enhancement was provided by the outcomes of experiments, particularly those involving the adsorption of iodine, methylene blue, and microscopic observations. The adsorbent's specific surface area was significantly enhanced by chemical activation. Based on the FTIR spectra (Figure 1), several peaks around 1000-1700 cm⁻¹ (C=O), 1500-1700 cm⁻¹ (C=C), 1000-1300 cm⁻¹ (C-O), 3400-4000 cm⁻¹ (O-H), could be observed in both samples. At first, the concentration was about 230 parts per million. The concentration of toluene dropped when the adsorbents encountered toluene-containing air. When the measured concentration changes are compared, there is a noticeable distinction between the activated and unactivated adsorbents. Over time, the concentration of the un-activated adsorbent dropped but eventually stabilized at 180-170 ppm. This finding suggests that after around 60 minutes of exposure, the level of adsorbed toluene stabilized. On the other hand, the toluene concentration decreased more noticeably and remained low for the duration of the observation for the K₂CO₃-activated adsorbent (0-120 min). The amount of toluene adsorbed on the activated adsorbent at equilibrium may have been significantly greater than that on the un-activated adsorbent, indicating that the toluene adsorption did not achieve equilibrium during the observation. As a result, activation with K₂CO₃ increased the adsorbents made from buckwheat hulls' ability to adsorb toluene.

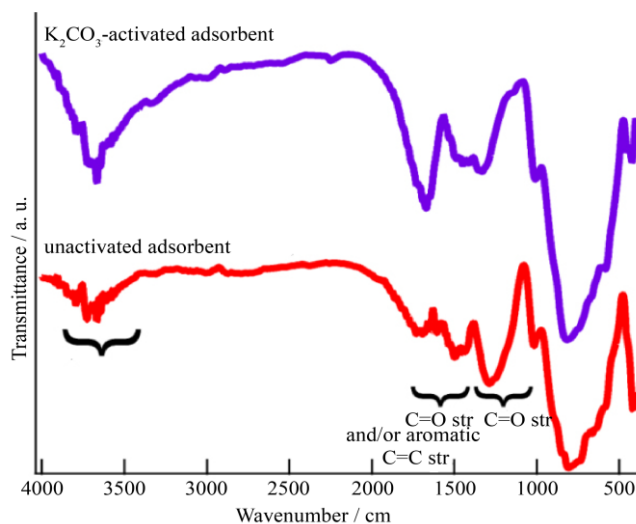


Fig. 1 FT-IR spectra of K₂CO₃-activated carbon (purple) and un-activated activated carbon (red). [30]

The introduction of mesopores through K_2CO_3 activation and the increase in specific surface area are congruent with this rise in the toluene adsorption capacity. Vohra and co-workers [30] evaluated the effectiveness of date palm-tree branch-derived activated carbon in treating gaseous toluene streams in a range of dynamic flow scenarios. The generated activated carbon exhibited a total pore volume of $0.437 \text{ cm}^3/\text{g}$, a micropore volume of $0.15 \text{ cm}^3/\text{g}$, an average pore width of 3.032 nm , and a specific surface area of $800.87 \text{ m}^2/\text{g}$.

The results show that these activated carbons can efficiently handle gaseous toluene under various working circumstances. It was observed that breakthrough and fatigue times increased with decreasing gas flow rate and concentration and increasing activated carbon bed depth. Response surface profiles demonstrated that at toluene gas influent concentrations of 10 and 20 ppmv, respectively, the toluene breakthrough time increased from 137 to 290 min and 70 to 146 min upon increasing the activated carbon column depth from 4 cm to 6 cm, while the exhaustion time increased from 300 to 437 min and 190 to 275 min.

These data imply that while the empty bed contact time increases with increasing column depth, throughput increases with higher volumes of toluene gas treated prior to breakthrough, leading to longer breakthrough and fatigue periods. Scanning Electron Microscopy (SEM) images reveal that the outer surfaces of the core and peel of maize straw are relatively smooth [31], in contrast to the rougher surfaces of cotton straw and pepper straw, which are due to their differing reactivity and the distribution of their components. The nitrogen (N_2) adsorption-desorption isotherms indicate that the maize straw peel displays typical characteristics of type I isotherms. As the vapor pressure approaches saturation, the isotherm steepens due to the presence of voids between particles, like microporous adsorption. The other four samples show similar behavior, with increased adsorption capacity at lower pressures and a concave curve.

The middle segment of the hysteresis loop indicates capillary condensation of the porous material, which falls under type IV isotherms (mesopores). From the studies on adsorption capacity, the order of toluene adsorption capacity from highest to lowest is reported (maize straw peel > millet straw > pepper straw > core of maize straw > cotton straw).

This suggests that the interaction between the adsorbent and the adsorbate, and the microporosity plays a significant role in adsorption capacity. In conclusion, the research team identified the optimal conditions for toluene adsorption as a carbonization temperature of $572 \text{ }^\circ\text{C}$, a carbonization time of 1.56 hours, and a carbon-to-bulk ratio of 1.60, with an estimated toluene adsorption capacity of 321.9 mg/g . Ordered Mesoporous Carbon (OMC) was created using a straightforward soft template approach [32] and then chemically activated with potassium hydroxide (KOH) to

develop complex pore structures. These mesopores are particularly good at enhancing the movement of substances, speeding up the adsorption of volatile organic compounds, and aiding in their release.

On the other hand, micropores are better at holding volatile organic compounds. The mesoporous carbon structure was successfully refined through the KOH activation, with BET-specific surface area and total pore volume reaching impressive values of $2661 \text{ m}^2\text{g}^{-1}$ and $2.14 \text{ cm}^3\text{g}^{-1}$, respectively. Transmission Electron Microscopy (TEM) revealed a structured pore system resembling wormholes in the ordered mesoporous carbon (Figure 2). Following the KOH activation, the mesopores maintained their structured, wormhole-like appearance, though the overall order of the pore structure in the sample slightly diminished.

Based on adsorption breakthrough curves, OMC showed the shortest breakthrough time (33 minutes) for toluene compared to other KOMC adsorbents, which took between 81 and 129 minutes. The KOMC adsorbents showed a gradual increase in adsorption capacity over time in the second phase of the toluene breakthrough curve, suggesting that the more microporous the structure, the more it hindered the mass transfer process.

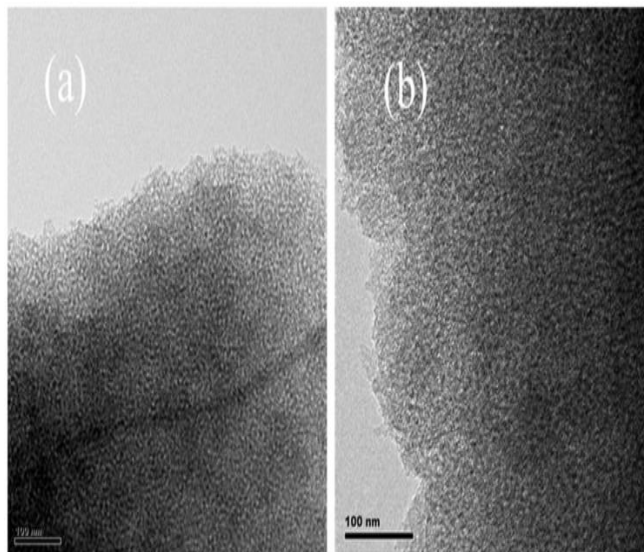


Fig. 2 TEM images of ordered mesoporous carbon (a) and KOH-modified activated carbon (b) [33].

Glycyrrhiza Glabra Root (GGR) is a waste material that removes toluene from gaseous solutions [33]. Shiraz, Iran-based Rishmak Inc., an extract manufacturer, supplied Glycyrrhiza glabra root. The herb's root was extracted at 140°C and 3.5 bar of pressure for two hours. After that, dewatered GGR is disposed of as waste throughout the company. The adsorbate concentration, temperature, humidity, and contact time varied during the batch adsorption experiments. The sorbent humidity was raised to fifty percent

to enhance the adsorption capacity. When the sorbent was saturated, the adsorption of toluene also increased over the course of the 12-hour contact period.

The adsorption data was better fitted by the pseudo-second-order kinetic model ($R^2=0.996$) and the Freundlich model ($R^2=0.992$) than by other kinetic and isotherm models, respectively. The Freundlich model is an empirical mathematical expression that outlines the correlation between the quantity of a gas or liquid adsorbed on a solid surface and the pressure or concentration of that substance in the nearby medium. It indicates the extent to which a substance will be adsorbed on a solid surface at a specific concentration, grounded in the concept that the adsorption sites on the surface lack uniformity and possess different adsorption energies. This model is especially effective for characterizing adsorption on uneven surfaces where the binding sites possess varying adsorption energies. The pseudo-second-order kinetic model is a mathematical expression that illustrates the adsorption of materials onto a surface.

It is a well-known model for adsorption kinetics due to its simplicity and ability to accommodate various systems. This model indicates that the adsorption rate is affected by the interaction among adsorption sites on the surface. The pseudo-second-order kinetic model is frequently employed to analyze data regarding the adsorption of dyes, metal ions and various compounds onto cellulose-derived substances. This model is likewise applied to simulate adsorption processes requiring considerable time to occupy adsorption sites. The physical nature of the sorption by GGR was further demonstrated by the Dubinin-Radushkevich isotherm.

The thermodynamic analysis showed that the adsorption process is exothermic, as indicated by the negative value of the adsorption enthalpy. An adsorption process is regarded as exothermic when adsorbate molecules adhere to the surface of the adsorbent. It lowers the surface energy of the systems, emitting heat and leading to a negative adsorption enthalpy value. It was noticed that the systems gain stability by releasing energy as adsorbate molecules bond to the surface, reducing their mobility.

With an entropy change value of $-150.48 \text{ J/mol}\cdot\text{K}$, the amount of adsorbed toluene released onto the adsorbent is reduced. In an adsorption process, entropy usually declines because the movement freedom of adsorbate molecules decreases upon adhering to the adsorbent surface, resulting in a more ordered system, leading to a negative change during the adsorption process.

While ΔG 's positive values suggested that sorption was not favorable at temperatures between 30 and 50 degrees Celsius, its negative values in the 10 to 25°C temperature range suggested that the adsorption process was spontaneous and feasible. As highlighted in literature by many researchers (Table 3), toluene removal could be carried out using activated carbon, which is prepared by various types of precursors. Activated carbon can be recycled via thermal activation, washing and other techniques. Recycling activated carbon is an eco-friendly method to decrease waste and preserve resources. The most prevalent technique for regenerating exhausted granular activated carbon. Entails subjecting carbon to elevated temperatures in a water vapor-rich environment. The charcoal can recover its initial capacity.

Table 3. Removal of toluene using activated carbon

Precursors	Properties of activated carbon and the adsorption data
Durian shell	<ol style="list-style-type: none"> The precursor was impregnated with phosphoric acid via carbonization (500 °C, 20 minutes) under a nitrogen atmosphere [34]. The highest BET surface area was 1404 m²/g. The highest removal efficiency of toluene vapors was observed using 30% phosphoric acid. Adsorption data obeyed the Freundlich model.
Coal	<ol style="list-style-type: none"> Adsorption data [35] supported the Langmuir-BET hybrid model ($R^2=0.99$).
Zanthoxylum bungeanum trees	<ol style="list-style-type: none"> Activated carbon [36] prepared at 650 °C showed unique properties (surface area=1006.2 m²/g, micro-mesoporous structure and mesoporous proportion of 65.5%). High temperature (100 °C) could destroy strong interaction between the oxygen atoms (functional groups) and the <i>p</i>-electrons (toluene). Adsorption capacity achieved 417 mg/g.
Palm fibers	<ol style="list-style-type: none"> The precursors were cleaned, ground, and sieved (1–2 mm). The sieved fiber was carbonized (450 °C, 300 min) in a vertical tubular reactor under nitrogen flow. EDX spectra confirmed that the main elements are carbon and oxygen [37]. Toluene removal efficiencies reached 90%.
Walnut shell	<ol style="list-style-type: none"> Activated carbon was produced through chemical activation (ZnCl_2) and carbonization stage (500°C). The highest yield was observed using an impregnation ratio of 1.5 wt/wt zinc chloride [38]. XRD analysis highlighted that peak intensity decreased when the impregnation ratio was increased. The largest surface area was 2643 m²·g⁻¹ using an impregnation ratio of 2/1. The amount of toluene adsorbed strongly depends on the physicochemical properties of adsorbents.

Corncob	<ol style="list-style-type: none"> 1. The highest adsorption capacity was 414.6 mg/g (impregnation ratio=1:1, carbonization temperature=550 °C, carbonization time=60 minutes). 2. Adsorption data matches Freundlich isotherm. 3. Zinc chloride was used as an activating agent [39].
Moringa Oleifera seeds, banana peel	<ol style="list-style-type: none"> 1. Ash, organic matter, pH, particle size and surface area were found to be 3.3%, 96.7%, 5.55, 1mm and 4.01 m²/g, respectively, when the precursor was Moringa Oleifera seeds [40]. 2. Ash, organic matter, pH, particle size and surface area were 11.3%, 88.7%, 5.87, 1mm and 1.856 m²/g, respectively, when the precursor was a banana peel. 3. The percentage of toluene removed from banana peel-based activated carbon (15 °C) was 46%. 4. The percentage of toluene removal onto Moringa Oleifera seeds based on activated carbon at 20 °C was 60%.
Coconut shell	<ol style="list-style-type: none"> 1. Chemical activation was conducted, and the activating agent was potassium acetate [41] 2. The starting material consisted of low ash, resulting in a high yield. 3. Moisture, volatile content, ash, and fixed carbon were 5.6%, 71.3%, 1.1% and 23.3%, respectively. 4. Porosity development in the presence of an activating agent during the chemical activation process. 5. Surface area (622 m²/g) and pore volume (0.31 cm³/g) were reported. 6. The removal of toluene was 85.6%. 7. Adsorption data obeyed the Langmuir model (R²=0.9988), with the highest adsorption capacity of 227.27 mg/g.
Corn bran	<ol style="list-style-type: none"> 1. Specific surface area was 1896 m²/g, and total pore volume reached 1.04 cm³/g after 15 days of microbial pretreatment (<i>Trichoderma viride</i>). 2. Saturated adsorption capacity achieved 237 mg/g (100 ppm toluene), which is 1.58 times that of corn bran without microbial [42].
Bamboo	<ol style="list-style-type: none"> 1. Prepared activated carbon showed superior mechanical strength, more stable (wet conditions), and higher carbon content. 2. Well-developed micropores adsorbent [43] indicated high adsorption capacity (up to 350 mg/g).
Watermelon rind	<ol style="list-style-type: none"> 1. Fixed carbon was 60% under the optimized conditions (temperature=500 °C, time=2.165 hours and impregnation ratio=2/1). 2. Sulphuric acid-treated samples (900.36 m²/g) indicated better results than zinc chloride. 3. It was noted that higher removal efficiency (22% for toluene) could be observed at lower temperatures [44].

4. Removal of Toluene Using Other Adsorbents

Textural properties such as specific surface area (75.59 m²/g), micropore volume (0.004 cm³/g), total pore volume (0.149 cm³/g), and average diameter of pores (7.39 nm) of Na-Pa zeolite was highlighted [45]. A higher correlation coefficient (R²) could be found in the pseudo-second-order (R²=0.999) and Langmuir model (R²=0.998), respectively. It was noted that zeolite can remove 55% of toluene at equilibrium conditions (within 24 hours). Zeolite is typically regarded as superior to fly ash due to its markedly higher adsorption capacity, allowing it to capture and eliminate pollutants such as heavy metals from water and soil more efficiently, thanks to its distinct porous design and ion exchange properties. At the same time, fly ash by itself has constrained adsorption ability.

USY (Si/Al = 11, 25, 40) zeolite was acquired from Zibo Mengzhong Import and Export Trade Co., Ltd. (Shandong, China). The cation type of USY was identified as hydrogen. Key features such as surface area (748-881 m²/g), micropore volume (0.284-0.315 cm³/g), external volume (0.124-0.15 cm³/g), and total pore volume (0.408-0.465 cm³/g) of the micro-mesopore structure of ultra-stable Y zeolite (USY)

were documented [46]. Experimental findings supported the observation that the breakthrough time was prolonged as the Si/Al ratios were increased at 50% relative humidity. It was observed that the USY exhibited outstanding adsorption capabilities and hydrophobicity at a Si/Al ratio of 40. Moreover, it was concluded that the removal efficiency reached 98.6% at a relative humidity of 50%. The feed flow rate also had a notable impact on the adsorption process. The time required for breakthrough decreased from 265 to 85 minutes as the feed flow rate escalated from 200 to 700 mL/min.

Concurrently, the adsorption capacity increased from 0.181 to 0.224 g/g. This outcome suggested that a higher feed flow rate improved the adsorption capacity of toluene. The adsorption isotherm was investigated, revealing a complex behavior characterized by both multilayer and homogeneous adsorption. The R² values of various adsorption isotherm models were ranked as Langmuir–Freundlich > Langmuir > Freundlich. Throughout the adsorption process, the adsorbent bed transitioned sequentially through a stable state, breakthrough state, and saturation state. In the stable state, the mass transfer zone remained within the adsorbent bed's

boundary. As toluene molecules were continuously adsorbed onto USY, the amount of toluene absorbed increased linearly with time. CuX materials (CuX-B1, CuX-B2, CuX-B3) were synthesized by ion exchange using commercial zeolite NaX (Si / Al = 1.3). NaX zeolite was replaced with copper nitrate solution.

The amount of copper transfer surface was evaluated, and it was assumed that one Cu^{2+} ion could replace two Na^+ ions in the zeolite. As shown in the size distribution studies (figure 3), the interaction of NaX zeolite with Cu solutions leads to the appearance of peaks in the mesoporous region at 6.5 and 4.5 nm for CuX-B2 samples and CuX-B3, respectively. It is noted that the exchange rate of Na^+ is not very high (less than 9%), and the increase in Cu content can explain this additional mesoporosity due to CuO species. Copper zeolites could be used for low-temperature toluene removal [47]. Specific surface area, pore volume and micropore volume were 384-434 m^2/g , 0.218-0.223 cm^3/g and 0.185-0.211 cm^3/g , respectively.

It was noted that specific surface area will be reduced when the copper content increases. XRD studies confirm that no new phase could be observed in copper-exchanged zeolite X samples if compared to the parent zeolite. However, the intensity of these peaks decreased, representing a certain loss of crystallinity in these samples. The longest breakthrough time (473 minutes) and highest adsorption capacity (22.2 g/100g solid) were found in the CuX-B1 sample.

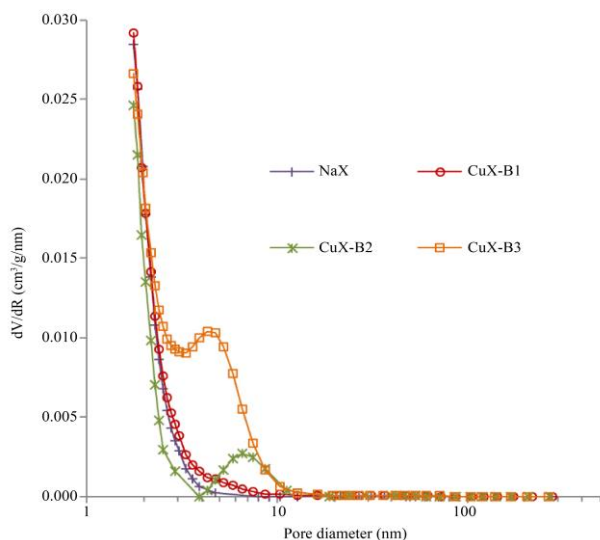


Fig. 3. Pore size distribution of prepared CuX-B materials and NaX zeolite [48]

Higher specific surface area [48] in the samples by modification with copper (2.7735 m^2/g) and nickel (2.6681 m^2/g) if compared to unmodified zeolite 4A (0.69296 m^2/g). The removal percentage increased when the time, pH and adsorbent dosage were increased, but the temperature was

reduced. The best experimental conditions, such as contact time (75 minutes), adsorbent dosage (5g), pH (pH 10), and temperature (25 °C), were highlighted. Adsorption data supported the Freundlich model and pseudo-second-order model. In addition, the adsorption process was exothermic and stable based on thermodynamic studies.

According to Deng and colleagues [49], USY (FAU, NaX zeolite) has a supercage structure and a high Si/Al ratio, making it the best option for selectively reducing toluene. Furthermore, they propose that, in humid environments, the silicalite-1 small-pore network is the most effective adsorbent for removing dichloromethane and toluene from the mixed exhaust. The structural characteristics of the prepared samples were examined using the X-Ray Diffraction (XRD) technique. At 2θ values of 6.1, 9.9, 11.7, 15.4, 23.31, and 26.6°, respectively, the main (1 1 1), (2 2 0), (3 1 1), (3 3 1), (5 3 3), and (6 4 2) reflections of NaX match the pattern of FAU zeolite (ICDD No. 01-072-2422). The results of the static adsorption equilibrium showed that micropore filling stabilizes toluene.

Mesoporous silica materials are characterized by a high specific surface area and exhibit excellent thermal and hydrothermal stability, making them widely utilized as adsorbents. The primary raw material for synthesising these mesoporous silica materials is silica. However, silica obtained from inorganic silicates tends to be costly [50]. Consequently, it is essential to identify an alternative silica source. In 1985, SiO_2 and Al_2O_3 were first extracted from coal fly ash through an alkaline hydrothermal reaction, subsequently facilitating microporous molecular sieves synthesis.

Following this, numerous studies have focused on producing mesoporous silica materials utilizing silica derived from coal fly ash [51]. Toluene adsorption onto mesoporous silica was conducted in a fixed-bed reactor with an inner diameter of 10 mm. Toluene gas was generated by introducing nitrogen into liquid toluene, while nitrogen and air served as balance gases to regulate the desired concentrations of toluene and oxygen. The oxygen content was maintained at 10%, with a volumetric flow rate of 500 sccm. Once the inlet concentrations of toluene and oxygen stabilized, the adsorption process commenced within the reactor.

As noted by Liu and Lan [52], the bottom ash from incineration will be utilized to create mesoporous silica materials characterized by a smooth surface and crystalline structure. The mesoporous volume, average pore diameter, and specific surface area were measured at 0.854 cm^3/g , 3.4 nm, and 992 m^2/g , respectively. Scanning Electron Microscopy (SEM) images revealed a crystalline structure with a smooth surface. Transmission Electron Microscopy (TEM) images suggested that the hexagonal pore arrangement of the mesoporous materials was not distinctly observable. This phenomenon can be attributed to the presence of various

metal impurities in the supernatant solution derived from the bottom ash. The researchers concluded that the adsorption capacity reached 124 mg/g at a temperature of 25 °C, with a toluene concentration of 1100 ppm. The findings indicated that the toluene adsorption capacity increased as the toluene concentration rose. Additionally, the results demonstrated that breakthrough times lengthened with an increase in the weight of the adsorbent, although the variation in toluene adsorption capacity remained minimal.

By using a two-stage variable temperature hydrothermal treatment [53], three different types of hierarchical Mordenite Framework Inverted (MFI)-type nanozeolites, namely Si-MFI, Al-MFI, and Ti-MFI, were successfully synthesized. Several techniques were employed to assess the adsorption characteristics of as-synthesized hierarchical zeolite samples using toluene as the probe molecule. These techniques included the use of toluene-TPD (temperature-programmed desorption of toluene), adsorption breakthrough curves, kinetics models, and simulation of adsorption isotherms. According to the results of the dynamic adsorption, Ti-MFI had the best toluene adsorption performance (45 mg/g_{ads}) in the wet gas condition (where the relative humidity was 50%), while Al-MFI had the highest toluene adsorption capacity (58 mg/g_{ads}) in the dry gas condition.

According to the simulation results, toluene's adsorption behavior on hierarchical MFI nanozeolites followed the Freundlich model ($R^2 > 0.96$) and pseudo-first-order isotherm ($R^2 > 0.9826$). Without any additional diffraction peaks, XRD patterns verified that all samples possessed the standard MFI microporous zeolite structure (JCPDS, PDF44-0003). Additionally, the Al-MFI and Ti-MFI cell parameters slightly increased when compared to the Si-MFI values, suggesting that the doping of Al and Ti into the zeolite lattice was successful. According to the FTIR investigations, the Si-MFI sample had a lower intensity of the adsorption peak, which suggested that it was more hydrophobic.

As-prepared Si-MFI, Al-MFI, and Ti-MFI had crystallinity percentages of 67%, 69%, and 61%, respectively. The as-synthesized zeolites have a BET surface area distribution of 294–362 m²/g. The single point adsorption volume at P/P₀ ¼ 0.985 yielded a total volume of 0.21 cm³/g for Si-MFI, 0.26 cm³/g for Al-MFI, and 0.21 cm³/g for Ti-MFI, respectively. SEM images demonstrated that spherical nanozeolite crystal aggregation with a smooth surface was clearly visible and that the interparticle of nanozeolite crystal aggregation produced a mesoporous structure. Si-MFI, Al-MFI, and Ti-MFI aggregated spherical nano zeolites had respective sizes of 500–700, 200–450, and 350–550 nm. According to TEM investigations, the agglomeration of nanosized zeolite particles produced the mesoporous structure present in all the as-prepared Si-MFI, Al-MFI, and

Ti-MFI. Furthermore, in agreement with the SEM, the samples' spherical morphology and diameter of roughly 300–500 nm were observed.

Examining the potential of cereals and crop residues as a substitute for fossil fuels is one of the current research projects. Finding cereal species and varieties with high biomass yields, high combustibility, low ash contents, and minimal boiler corrosion potential is of utmost importance. As an alternative energy source, annual crops (wheat, rye, and triticale) are grown because they don't need a lot of capital and can simply rotate through the crop cycle. Techniques for cultivation, fertilization, and harvesting are necessary to guarantee the most efficient use of resources. Rye and triticale are, therefore, superior to wheat in this regard since they have lower grain losses and need less pesticides, fertilizers, and insecticides. For energy crops, emissions and efficiency were essentially the same as for wheat straw.

For some plants, burning releases nitrogen from the grain's protein content, resulting in a noticeable increase in NO_x emissions. In addition, the high alkali content of the fuel, which can cause corrosion in boilers, and the high concentration of heavy metals in the ashes, which prohibit their spreading over farmland, need to be considered. Because of their high potassium content, the ashes from burning crops with coal cannot be used in the cement industry. The need for farmers to produce at a profit and the market prices projected by energy strategies appear to diverge significantly in terms of hard economic realities.

Ghiachi and co-workers [54] reported using wheat ash (barley, barley, triticale and wheat grains) for toluene removal. SEM analysis confirmed that wheat, barley and oat ash have similar structures after calcination. The composition of triticale ash is different from other grains. The aleurone cells become very disorganized, and lesions appear when all parts of the aleurone cells and associated endosperm are missing. The level of wheat ash is low, between 2 to 6 m²/g. The adsorption experiments show that the adsorption capacity increases with increasing equilibrium concentration. Increasing the loading capacity of catalysts and increasing the concentration of toluene is due to the interaction between toluene and catalysis. Toluene adsorption isotherms can be classified as type C of the Giles classification of adsorption isotherms. The adsorbent's nature means there is no strong bond between the toluene and the adsorbent. The Freundlich isotherm model, a common model for aqueous-phase adsorption, was used to fit the experimental adsorption equilibrium data of organic pollutants on cereal ashes. The adsorption equilibrium between an adsorbate in solution and the adsorbent surface is represented by the Freundlich model. The Freundlich constant (described as the adsorption capacity) was found to be 0.04 mg/g, 0.0051 mg/g,

0.042 mg/g and 0.032 mg/g, for oat, wheat, triticale and barley, respectively. Fly ash is classified as an industrial byproduct resulting from coal combustion, consisting of fine particulate matter [55]. The rapid pace of industrialization and the increasing electricity demand have resulted in the annual release of hundreds of millions of tons of fly ash globally, with approximately 80% of this material being fly ash itself. While coal-fired power generation is essential for providing energy to both residential and industrial sectors, it simultaneously contributes to air and water pollution, thereby disrupting ecological systems.

When released untreated from power plant stacks, fly ash poses significant risks to atmospheric quality and human health. Nevertheless, advancements in science and technology are transforming fly ash from mere industrial waste into valuable raw material. Characterized by a large porous structure and irregular shape, fly ash possesses extensive specific surface areas and notable adsorption capabilities.

The properties of fly ash are primarily influenced by the type of coal used and the conditions under which it is combusted. Fly ash is much less expensive than activated carbon, making it a more economical choice as an adsorbent in different applications because of its abundant availability and status as a waste product. Zeolite can undergo recycling through multiple methods, such as reusing natural zeolites, reclaiming spent FCC catalysts and producing zeolites from waste substances. Natural zeolites can be used again in composting methods to extract heavy metals from sewage sludge. The frequency of natural zeolite reuse can be evaluated by observing the variation in heavy metal levels in the compost. Used FCC catalysts can undergo a multi steps leaching procedure to reclaim metal impurities. The solid by-products can subsequently be used to produce zeolite ZSM-5.

Fortunately, fly ash is recyclable and can be reused, with over 22 million tons utilized each year across various engineering applications. Fly ash can be reused to create various products, such as construction materials, zeolites and aerogels. Fly ash can serve as cement and brick. Fly ash may serve as an alternative material for cement, which is the main component of concrete. For each ton of fly ash used instead of Portland cement, approximately one ton of carbon dioxide is kept from being released into the earth's atmosphere. Fly ash uses less water compared to Portland cement, decreases energy usage, and minimizes the demand for landfill capacity.

5. Treatment of Industrial Wastewater

In Bangladesh, a significant amount of the rice husk is discarded as a by-product during rice processing. Activated carbons are commonly used for adsorption, but their production expenses remain high. An adequate quantity of high-quality activated carbon was generated from rice husk, which was gathered from the local market and sun-dried. For textile wastewater treatment, the prepared activated carbon

had an adsorption capacity of 81%, while the commercial activated carbon showed 63% during the same period.

Consequently, the prepared activated carbon could have significant uses in the treatment of wastewater for its recycling and preservation. It was noted that it was sourced from a textile dyeing and washing facility, Sharoj Washing and Dyeing Ltd. Bangladesh [56]. Textiles may pose risks because of the prevalent use of hazardous chemicals in their production, which can contaminate water supplies, endanger workers, and lead to health problems for consumers via skin exposure, especially in cases where chemicals are involved.

Numerous chemicals involved in textile production, such as dyes, finishing agents, and pesticides applied to cotton crops, may be carcinogenic, disrupt endocrine functions and lead to skin irritation or allergic reactions upon skin contact. Significant quantities of wastewater with these substances are frequently discharged into water bodies during dyeing and finishing processes, negatively impacting organisms and interfering with ecosystems.

The wastewater samples for this study were collected from a sewing thread manufacturing factory [57] situated at 2°15'20.66"N latitude and 102°8'40.10"E longitude in Malacca, approximately one kilometer from the South Malacca Sea. The new wastewater samples were gathered from the influent collection of the factory's wastewater treatment facility after production's off-peak hours utilizing an eighty-one-liter plastic container in zeolite treatment. The elimination of heavy metals from a textile wastewater sample is significant, with the removal percentage exceeding 50% of the original concentration.

The rate of heavy metal elimination in textile water varies with zeolite and different alum concentrations. Copper (64.74%) was the most significant metal eliminated by zeolite, followed by chromium (56.26%) and lead (55.34%), while cadmium had the lowest removal rate at 50.20%. Conversely, the inclusion of zeolite with 10 mg/L alum resulted in a greater removal of heavy metals from the textile wastewater sample compared to using zeolite by itself. Heavy metals can be extracted from textile wastewater samples by as much as 80% for metals like cadmium and copper.

The presence of adsorption relies on the charge densities of the cations. The heavy metal cations examined are lead, copper, cadmium and chromium ions. All the cations of heavy metals exist as hexa-aqua complex ions in the solution and travel through zeolite in the hydrated state. The outcome demonstrated that the percentage of removal of cadmium by zeolite is the lowest, which is confirmed by the dimensions of cadmium cations. Even though charge densities for cadmium exceed those of copper and chromium cations, it seems that the diameter of hydrated cadmium ions is larger, resulting in minimal adsorption.

Biological Aerated Filters (BAF) are characterized by an attached growth method on fixed media during regular functioning with aeration. The primary aims of these processes were to achieve carbon oxidation and solid filtration. When BAF technology is utilized for treating industrial wastewater, choosing appropriate granular media is crucial for sustaining a significant level of active biomass and diverse microbial communities. Employing media that possess adsorption capacity can enable a method for combining biological removal and adsorption.

The use of BAF for treating textile wastewater with natural zeolite as the medium has been documented. Natural zeolite possesses the ability to absorb organic compounds and can also engage in cation exchange, such as with NH_4^+ ions. The textile industry's wastewater was introduced to the lab- and pilot-scale downflow biofilters, and the effectiveness of biofilters utilizing natural zeolites and sand media was monitored. The wastewater employed for the laboratory experiment was sourced from the J textile factory located in Seoul, Korea.

The fibers utilized in the textile sector can be categorized into two groups: natural and synthetic. The primary natural fibers are wool and cotton. The latter encompasses polyester, nylon, polyacrylic and polyamide. Between March and September 1998, raw textile wastewater samples were gathered each month in 20-liter plastic containers that had previously been cleaned and rinsed with distilled water. A pilot scale BAF utilizing natural zeolite, capable of treating up to $12\text{m}^3/\text{day}$ of textile wastewater, was observed for a duration

of 5 months. This system managed to eliminate approximately 99% of biochemical oxygen demand, 92% of chemical oxygen demand, 74% of suspended solids and 92% of T-N with a hydraulic load of $1.83\text{m}^3/\text{m}^2\text{h}$. Operating at a higher hydraulic load ($2.3\text{m}^3/\text{m}^2\text{h}$) and lower temperatures ($4\text{-}10\text{ }^\circ\text{C}$) led to a decrease in T-N removal efficiency, although the reduction in organic matter remained relatively unaffected [58].

Future studies on adsorbents (activated carbon, fly ash, zeolite) could emphasize enhancing manufacturing techniques, creating innovative nanomaterials and real-world applications. Challenges in industrial wastewater treatment should be identified and solved.

6. Conclusion

Toluene is a toxic chemical that should be removed from wastewater. Exposure to toluene can result in unhealthy effects on the human body and aquatic organisms. This work reported the removal of toluene from the activated carbon, zeolite, and fly ash. Removal efficiency was highlighted based on previous literature. Adsorption data could be described using the Langmuir model or Freundlich isotherm.

Funding Statement

One of the authors (Ho SM) was financially supported by INTI International University, Malaysia.

Acknowledgments

This research work was financially supported by INTI International University (Ho SM).

References

- [1] Samira Karimi, Mohammad Tavakkoli Yaraki, and Rama Rao Karri, "A Comprehensive Review of the Adsorption Mechanisms and Factors Influencing the Adsorption Process from the Perspective of Bioethanol Dehydration," *Renewable and Sustainable Energy Reviews*, vol. 107, pp. 535-553, 2019. [[CrossRef](#)] [[Google Scholar](#)] [[Publisher Link](#)]
- [2] Youssef Miyah et al., "MOF-Derived Magnetic Nano Composites as Potential Formulations for the Efficient Removal of Organic Pollutants from Water via Adsorption and Advanced Oxidation Processes: A Review," *Materials Today Sustainability*, vol. 28, 2024. [[CrossRef](#)] [[Google Scholar](#)] [[Publisher Link](#)]
- [3] Bellahsen Naoufal et al., "Adsorption of Nutrients Using Low-Cost Adsorbents from Agricultural Waste and by-Products-Review," *Progress in Agricultural Engineering Sciences*, vol. 14, no. 1, pp. 1-30, 2018. [[CrossRef](#)] [[Google Scholar](#)] [[Publisher Link](#)]
- [4] Sina Esfandiari Pour, Alireza Haghighat Mamaghani, and Zaher Hashisho, "Modeling of Adsorption Process on Monolith Adsorbents: A Mini-Review," *Separation and Purification Technology*, vol. 354, no. 2, pp. 1-18, 2025. [[CrossRef](#)] [[Google Scholar](#)] [[Publisher Link](#)]
- [5] Lu Cai et al., "Effective Adsorption of Diesel Oil by Crab-Shell-Derived Biochar Nanomaterials," *Materials*, vol. 12, no. 2, pp. 1-15, 2019. [[CrossRef](#)] [[Google Scholar](#)] [[Publisher Link](#)]
- [6] Sameena N. Malik et al., "Hybrid Ozonation Process for Industrial Wastewater Treatment: Principles and Applications: A Review," *Journal of Water Process Engineering*, vol. 35, 2020. [[CrossRef](#)] [[Google Scholar](#)] [[Publisher Link](#)]
- [7] Md. Shahinoor Islam, Hridoy Roy, and Sadiya Afrose, "Phosphoric Acid Surface Modified Moringa Oleifera Leaves Biochar for the Sequestration of Methyl Orange from Aqueous Solution: Characterizations, Isotherm, and Kinetics Analysis," *Remediation*, vol. 32, no. 4, pp. 281-298, 2022. [[CrossRef](#)] [[Google Scholar](#)] [[Publisher Link](#)]
- [8] Mohammad Mehdi Amin, Hassan Hashemi, and Amir Mohammadi Bovini, "A Review on Wastewater Disinfection," *International Journal of Environmental Health Engineering*, vol. 2, no. 1, pp. 1-9, 2013. [[CrossRef](#)] [[Google Scholar](#)] [[Publisher Link](#)]
- [9] Brieuc Verougstraete et al., "Advancements and Challenges in Electric Heating for Enhanced Temperature Swing Adsorption Processes," *Separation and Purification Technology*, vol. 353, part C, 2025. [[CrossRef](#)] [[Google Scholar](#)] [[Publisher Link](#)]

- [10] Siti Nur Fatimah Moideen et al., “Dual Phase Role of Composite Adsorbents Made from Cockleshell and Natural Zeolite in Treating River Water,” *Journal of King Saud University-Science*, vol. 32, no. 1, pp. 1-6, 2020. [[CrossRef](#)] [[Google Scholar](#)] [[Publisher Link](#)]
- [11] N. Bellahsen et al., “Pomegranate Peel as a New Low-Cost Adsorbent for Ammonium Removal,” *International Journal of Environmental Science and Technology*, vol. 18, no. 3, pp. 711-722, 2021. [[CrossRef](#)] [[Google Scholar](#)] [[Publisher Link](#)]
- [12] Hadid Sukmana et al., “Adsorption and Coagulation in Wastewater Treatment-Review,” *Progress in Agricultural Engineering Sciences*, vol. 17, no. 1, pp. 49-68, 2021. [[CrossRef](#)] [[Google Scholar](#)] [[Publisher Link](#)]
- [13] Ting Yang, and Aik Chong Lua, “Characteristics of Activated Carbons Prepared from Pistachio-Nut Shells by Physical Activation,” *Journal of Colloid and Interface Science*, vol. 267, no. 2, pp. 408-417, 2003. [[CrossRef](#)] [[Google Scholar](#)] [[Publisher Link](#)]
- [14] Tatsuru Goto et al., “Effect of Polarity of Activated Carbon Surface, Solvent and Adsorbate on Adsorption of Aromatic Compounds from Liquid Phase,” *Chemical and Pharmaceutical Bulletin*, vol. 63, pp. 726-730, 2015. [[CrossRef](#)] [[Google Scholar](#)] [[Publisher Link](#)]
- [15] Xiaodong Tang, Meijun Yao, and Jingjing Li, “Boric Acid-Modified Activated Carbon for Glycerol Removal from High-Salt Wastewater,” *Applied Surface Science*, vol. 670, 2024. [[CrossRef](#)] [[Google Scholar](#)] [[Publisher Link](#)]
- [16] Shane A. Snyder et al., “Role of Membranes and Activated Carbon in the Removal of Endocrine Disruptors and Pharmaceuticals,” *Desalination*, vol. 202, no. 1-3, pp. 156-181, 2007. [[CrossRef](#)] [[Google Scholar](#)] [[Publisher Link](#)]
- [17] Kshaf Azam et al., “A Review on Activated Carbon Modifications for the Treatment of Wastewater Containing Anionic Dyes,” *Chemosphere*, vol. 306, 2022. [[CrossRef](#)] [[Google Scholar](#)] [[Publisher Link](#)]
- [18] Maisa El Gamal et al., “Bio-Regeneration of Activated Carbon: A Comprehensive Review,” *Separation and Purification Technology*, vol. 197, pp. 345-359, 2018. [[CrossRef](#)] [[Google Scholar](#)] [[Publisher Link](#)]
- [19] Xiaoju Xiao et al., “Synthesis of Activated Carbon Loaded Nanosilver and Study of Water Corrosion Resistance and Antimicrobial Properties,” *Surfaces and Interfaces*, vol. 52, 2024. [[CrossRef](#)] [[Google Scholar](#)] [[Publisher Link](#)]
- [20] S. Shazia Shabir et al., “High Carbon Content Microporous Activated Carbon from Thin Walnut Shells: Optimization, Physico-Chemical Analysis and Structural Profiling,” *Process Safety and Environmental Protection*, vol. 190, pp. 85-96, 2024. [[CrossRef](#)] [[Google Scholar](#)] [[Publisher Link](#)]
- [21] Jianan Feng et al., “Synchronous Removal of Gaseous Toluene and Benzene and Degradation Process Shifts in Microbial Fuel Cell-Biotrickling Filter System,” *Bioresour. Technol.*, vol. 400, 2024. [[CrossRef](#)] [[Google Scholar](#)] [[Publisher Link](#)]
- [22] Pan-Yue Ni et al., “Biochar Enhanced the Stability of Toluene Removal in Extracted Groundwater Amended with Nitrate under Microaerobic Conditions,” *Chemosphere*, vol. 353, 2024. [[CrossRef](#)] [[Google Scholar](#)] [[Publisher Link](#)]
- [23] Statista, Market Volume of Toluene Worldwide from 2015 to 2022, with a Forecast for 2023 to 2030 (in Million Metric Tons), 2023. [Online]. Available: <https://www.statista.com/statistics/1245224/toluene-market-volume-worldwide/#:~:text=In%202022%2C%20the%20global%20market,worldwide%20in%20the%20year%202030>.
- [24] OEC, Toluene 290230 (Harmonized System 1992 for 6-digit), 2023. [Online]. Available: <https://oec.world/en/profile/hs/toluene>
- [25] Yong Zhu, Detao Xiao, and Xiangyuan Deng, “Study on the Regeneration of Activated Carbon Adsorbed with Radon by Using a Deep Depressurization Method,” *Radiation Medicine and Protection*, vol. 5, no. 4, pp. 260-267, 2024. [[CrossRef](#)] [[Google Scholar](#)] [[Publisher Link](#)]
- [26] Nabila Eka Yuningsih et al., “Adsorption of Malachite Green Using Activated Carbon from Mangosteen Peel: Optimization Using Box-Behnken Design,” *Journal of Renewable Materials*, vol. 12, no. 5, pp. 1-12, 2024. [[CrossRef](#)] [[Google Scholar](#)] [[Publisher Link](#)]
- [27] Qi Gao et al., “Innovative Green Preparation of Activated Carbon by Combining Microwave Pyrolysis and Self-Activation: Pyrolysis Behavior, Carbon Characteristics and Arsenic Adsorption Properties,” *Industrial Crops and Products*, vol. 220, 2024. [[CrossRef](#)] [[Google Scholar](#)] [[Publisher Link](#)]
- [28] Dariush Jafari, Morteza Esfandiyari, and Mehdi Mojahed, “Optimization of Removal of Toluene from Industrial Wastewater Using RSM Box-Behnken Experimental Design,” *Sustainable Environment Research*, vol. 33, pp. 1-11, 2023. [[CrossRef](#)] [[Google Scholar](#)] [[Publisher Link](#)]
- [29] Tomoya Takada, Ryo Tanaka, and Ryoto Ono, “Removal of Volatile Toluene Using K₂CO₃-Activated Carbon Adsorbents Prepared from Buckwheat Hull,” *Pollutants*, vol. 2, no. 1, pp. 12-20, 2022. [[CrossRef](#)] [[Google Scholar](#)] [[Publisher Link](#)]
- [30] Muhammad Vohra, Mohammad Al-Suwaiyan, and Minaam Hussaini, “Gas Phase Toluene Adsorption Using Date Palm-Tree Branches Based Activated Carbon,” *International Journal of Environmental Research and Public Health*, vol. 17, no. 24, pp. 1-18, 2020. [[CrossRef](#)] [[Google Scholar](#)] [[Publisher Link](#)]
- [31] Zhen Li, Yonghong Li, and Jiang Zhu, “Straw-Based Activated Carbon: Optimization of the Preparation Procedure and Performance of Volatile Organic Compounds Adsorption,” *Materials*, vol. 14, no. 12, pp. 1-16, 2021. [[CrossRef](#)] [[Google Scholar](#)] [[Publisher Link](#)]
- [32] Zhaohui An et al., “Synthesis and Adsorption Performance of a Hierarchical Micro-Mesoporous Carbon for Toluene Removal under Ambient Conditions,” *Materials*, vol. 13, no. 3, pp. 1-13, 2020. [[CrossRef](#)] [[Google Scholar](#)] [[Publisher Link](#)]
- [33] Fazel Mohammadi-Moghadam et al., “Application of Glycyrrhiza glabra Root as a Novel Adsorbent in the Removal of Toluene Vapors: Equilibrium, Kinetic, and Thermodynamic Study,” *Journal of Environmental and Public Health*, vol. 2013, pp. 1-7, 2013. [[CrossRef](#)] [[Google Scholar](#)] [[Publisher Link](#)]

- [34] Y.J. Tham et al., “Performances of Toluene Removal by Activated Carbon Derived from Durian Shell,” *Bioresource Technology*, vol. 102, no. 2, pp. 724-728, 2011. [[CrossRef](#)] [[Google Scholar](#)] [[Publisher Link](#)]
- [35] F. Zeinali, A.A. Ghoreyshi, and G. Najafpour, “Removal of Toluene and Dichloromethane from Aqueous Phase by Granular Activated Carbon (GAC),” *Chemical Engineering Communications*, vol. 199, no. 2, pp. 203-220, 2012. [[CrossRef](#)] [[Google Scholar](#)] [[Publisher Link](#)]
- [36] Guizhi Zhang et al., “Activated Carbon Adsorbents with Micro-Mesoporous Structure Derived from Waste Biomass by Stepwise Activation for Toluene Removal from Air,” *Journal of Environmental Chemical Engineering*, vol. 9, no. 4, 2021. [[CrossRef](#)] [[Google Scholar](#)] [[Publisher Link](#)]
- [37] F. Alshahrani et al., “Removal of Benzene, MTBE and Toluene from Contaminated Waters Using Biochar-Based Liquid Activated Carbon,” *Scientific Reports*, vol. 12, no. 1, pp. 1-11, 2022. [[CrossRef](#)] [[Google Scholar](#)] [[Publisher Link](#)]
- [38] Leila Karimnezhad, Mohammad Haghghi, and Esmail Fatehifar, “Adsorption of Benzene and Toluene from Waste Gas Using Activated Carbon Activated by $ZnCl_2$,” *Frontiers of Environmental Science & Engineering*, vol. 8, pp. 835-844, 2014. [[CrossRef](#)] [[Google Scholar](#)] [[Publisher Link](#)]
- [39] Jiang Zhu et al., “Removal of Toluene from Waste Gas by Adsorption-Desorption Process Using Corncob-Based Activated Carbons as Adsorbents,” *Ecotoxicology and Environmental Safety*, vol. 165, pp. 115-125, 2018. [[CrossRef](#)] [[Google Scholar](#)] [[Publisher Link](#)]
- [40] Rahima A, “Evaluation of Benzene, Toluene and p-Xylene Removal from Produced Water Using Locally Available Adsorbents and Granular Activated Carbon,” *International Research Journal of Engineering and Technology*, vol. 7, no. 9, pp. 2619-2639, 2020. [[Google Scholar](#)] [[Publisher Link](#)]
- [41] J. Mohammed, U.D. Hamza, A. Garba, “Potassium Acetate-Coconut Shell Activated Carbon for Adsorption of Benzene and Toluene: Equilibrium and Kinetic Studies,” *Nigerian Journal of Tropical Engineering*, vol. 16, no. 1, pp. 1-17, 2022. [[Google Scholar](#)] [[Publisher Link](#)]
- [42] Xiaohong Wang et al., “Preparation of Porous Carbon Based on Partially Degraded Raw Biomass by *Trichoderma Viride* to Optimize its Toluene Adsorption Performance,” *Environmental Science and Pollution Research*, vol. 28, pp. 46186-46195, 2021. [[CrossRef](#)] [[Google Scholar](#)] [[Publisher Link](#)]
- [43] Lijuan Hu et al., “Monolithic Bamboo-Based Activated Carbons for Dynamic Adsorption of Toluene,” *Journal of Porous Materials*, vol. 24, pp. 541-549, 2017. [[CrossRef](#)] [[Google Scholar](#)] [[Publisher Link](#)]
- [44] Chiemeka Ijeoma Korie, “Development of Watermelon Rind Activated Carbon for Removal of Benzene and Toluene from Oil Wastewater,” PhD Theses, University of Technology, 2021. [[Google Scholar](#)]
- [45] Lidia Bandura, Dorota Kołodyńska, and Wojciech Franus, “Adsorption of BTX from Aqueous Solutions by Na-P1 Zeolite Obtained from Fly Ash,” *Process Safety and Environmental Protection*, vol. 109, pp. 214-223, 2017. [[CrossRef](#)] [[Google Scholar](#)] [[Publisher Link](#)]
- [46] Lei Xu et al., “Removal of Toluene by Adsorption/Desorption Using Ultra-stable Y Zeolite,” *Transactions of Tianjin University*, vol. 25, pp. 312-321, 2019. [[CrossRef](#)] [[Google Scholar](#)] [[Publisher Link](#)]
- [47] Douglas Romero et al., “Removal of Toluene over NaX Zeolite Exchanged with Cu^{2+} ,” *Catalysts*, vol. 5, no. 3, pp. 1479-1497, 2015. [[CrossRef](#)] [[Google Scholar](#)] [[Publisher Link](#)]
- [48] Zahra Mamaghanifar et al., “BTX Removal from Aqueous Solution Using Copper- and Nickel-Modified Zeolite 4A: Kinetic, Thermodynamic, and Equilibrium Studies,” *Water Conservation Science and Engineering*, vol. 5, pp. 1-13, 2020. [[CrossRef](#)] [[Google Scholar](#)] [[Publisher Link](#)]
- [49] Hua Deng et al., “Adsorptive Removal of Toluene and Dichloromethane from Humid Exhaust on MFI, BEA and FAU Zeolites: An Experimental and Theoretical Study,” *Chemical Engineering Journal*, vol. 394, 2020. [[CrossRef](#)] [[Google Scholar](#)] [[Publisher Link](#)]
- [50] Jie-feng Wu et al., “Modeling of Effect of Fly Ash Amount on Microstructure and Chloride Diffusivity of Blended Fly Ash-Cement Systems,” *Construction and Building Materials*, vol. 443, 2024. [[CrossRef](#)] [[Google Scholar](#)] [[Publisher Link](#)]
- [51] Yongqiang Hou et al., “Optimizing Mechanical Performance and Flow Characteristics of Alkaline Fly Ash/Rice Husk Ash Composite Backfill: Insights from Multi-Factor Analysis and Engineering Optimization,” *Journal of Building Engineering*, vol. 95, 2024. [[CrossRef](#)] [[Google Scholar](#)] [[Publisher Link](#)]
- [52] Zhen-Shu Liu, and Hai-Ming Lan, “Synthesis of Mesoporous Silica Materials from Incineration Bottom Ash for the Removal of Toluene,” *International Journal of Environmental Science and Development*, vol. 10, no. 3, pp. 96-99, 2019. [[CrossRef](#)] [[Google Scholar](#)] [[Publisher Link](#)]
- [53] Shushu Huang et al., “Adsorptive Properties in Toluene Removal over Hierarchical Zeolites,” *Microporous and Mesoporous Materials*, vol. 302, pp. 1-10, 2020. [[CrossRef](#)] [[Google Scholar](#)] [[Publisher Link](#)]
- [54] M. Ghiaci et al., “Adsorption of Organic Pollutants from Aqueous Solutions on Cereal Ashes,” *Journal of Chemical & Engineering Data*, vol. 53, no. 11, pp. 2707-2709, 2008. [[CrossRef](#)] [[Google Scholar](#)] [[Publisher Link](#)]
- [55] Jun Cong Ge, Sam Ki Yoon, and Nag Jung Choi, “Application of Fly Ash as an Adsorbent for Removal of Air and Water Pollutants,” *Applied Sciences*, vol. 8, no. 7, pp. 1-24, 2018. [[CrossRef](#)] [[Google Scholar](#)] [[Publisher Link](#)]

- [56] M. Mahmudur Rahman et al., “An Approach to Producing Activated Carbon from Rice Husk for Treatment of Coloured Wastewater,” *Proceedings of the International Conference on Global Ecosystems, Biodiversity and Environmental Sustainability in the 21st Century*, Assam University, pp. 1-10, 2012. [[Google Scholar](#)]
- [57] Normala Halimoon, and Rachel Goh Soo Yin, “Removal of Heavy Metals from Textile Wastewater Using Zeolite,” *Environmental Asia*, vol. 3, pp. 124-130, 2010. [[Google Scholar](#)] [[Publisher Link](#)]
- [58] Won-Seok Chang, Seok-Won Hong, and Joonkyu Park, “Effect of Zeolite Media for the Treatment of Textile Wastewater in a Biological Aerated Filter,” *Process Biochemistry*, vol. 37, no. 7, pp. 693-698, 2022. [[CrossRef](#)] [[Google Scholar](#)] [[Publisher Link](#)]